Title
CLASSICAL AND QUANTUM MECHANICAL STUDIES OF HF IN AN INTENSE LASER FIELD

Authors
Dardi, P.S.
Gray, S.K.

Publication Date
1982-02-01

LBL-14060
Preprint

Lawrence Berkeley Laboratory
UNIVERSITY OF CALIFORNIA

Materials & Molecular
Research Division

Submitted to the Journal of Chemical Physics

CLASSICAL AND QUANTUM MECHANICAL STUDIES OF HF IN AN INTENSE LASER FIELD

Peter S. Dardi and Stephen K. Gray

February 1982

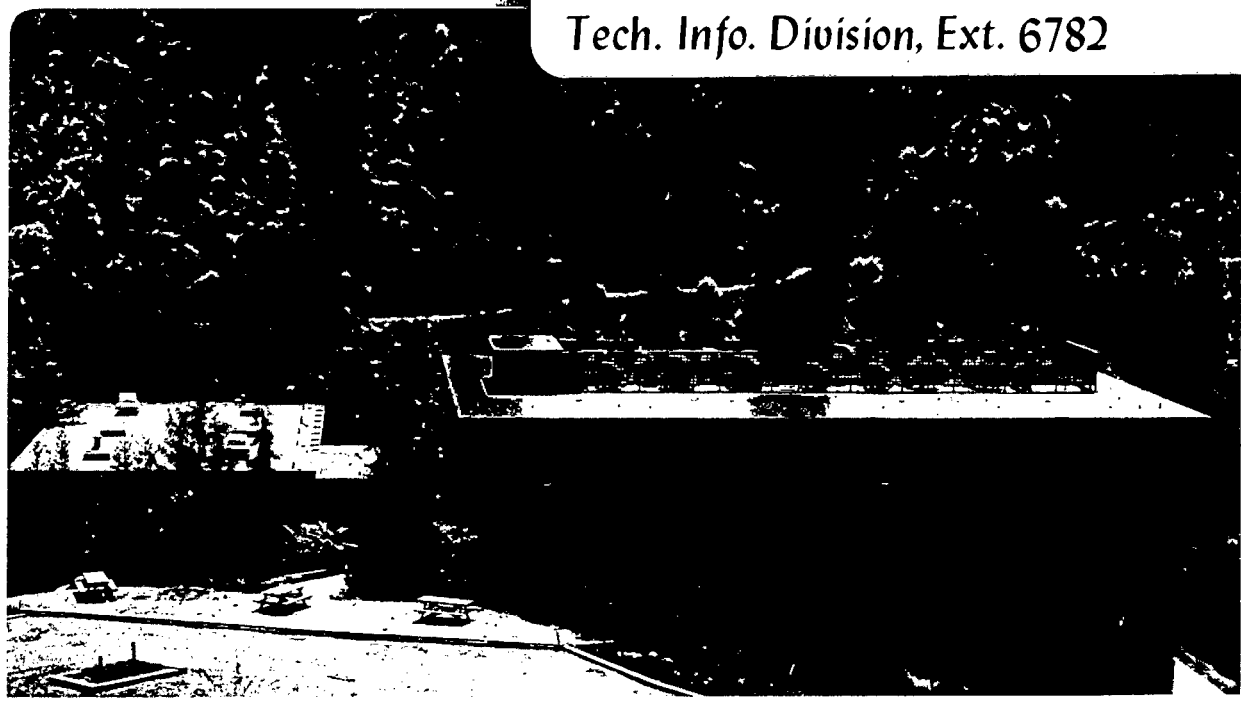

Prepared for the U.S. Department of Energy under Contract DE-AC03-76SF00098

DISCLAIMER

Classical and Quantum Mechanical Studies of HF in an Intense Laser Field

Peter S. Dardi and Stephen K. Gray

Department of Chemistry, and Materials and Molecular Research Division,
of the Lawrence Berkeley Laboratory, University of California,
Berkeley, California 94720

This work was supported by the Director, Office of Energy Research, Office of Basic Energy Sciences, Chemical Sciences Division of the U.S. Department of Energy under Contract Number DE-AC03-76SF00098; and in part by the National Science Foundation under grant number CHE-79-20181.

Abstract

The behavior of an HF molecule in an intense laser field is investigated with both classical trajectories and quantum dynamics. Vibration-rotation transition probabilities and energy absorption as a function of laser pulse time are calculated for the diatomic initially in its ground state. For comparison, results are also reported for a model non-rotating HF molecule. It is found that classical mechanics does not predict the correct time behavior of the system, nor does it predict the correct rotational state distributions. Classical mechanics does, however, predict pulse time averaged quantities to be the correct order of magnitude. There is also a correct general trend of increased multiphoton excitation for laser frequencies red-shifted from the one-photon resonance, although multiphoton resonance peaks are not observed in the classical results and far too little multiphoton excitation is predicted. The effect of laser phase has also been investigated and shown to be relatively unimportant in both the classical and quantum dynamics.

I. Introduction

With the development of high powered infrared lasers, much interest has been focused on the interaction of molecular systems with intense infrared radiation.[1] To understand theoretically how molecules absorb energy under such conditions requires a nonperturbative analysis. Because of the many degrees of freedom in even small polyatomic molecules, an accurate solution of the time-dependent Schrödinger equation is not, at present, possible for most molecules of experimental interest. Classical trajectory models, however, can be constructed and solved for model polyatomics interacting with radiation,[2] although there remain serious difficulties in defining accurate potential surfaces and in numerically integrating large numbers of coupled, nonlinear equations over the relevant time scale for absorption. It is therefore important to understand the limitations and accuracy of classical models.

The simplest, realistic system to study is a diatomic molecule interacting with a laser. Accurate, numerical classical and quantum solutions may be obtained for this problem. Because of the small number of quantum states involved, this represents a particularly severe test of classical mechanics. Previously, Walker and Preston[3] have performed both quantum and classical calculations for a model, non-rotating HF molecule. Their results, with laser intensities $\gtrsim 10$ TW/cm^2 (1TW = 10^{12} Watts), indicated good agreement between classical and quantum predictions of energy absorption averaged over laser pulse times, except near multiphoton resonances. Various other aspects of the problem of a diatomic interacting with a laser have been examined using either classical[4] or quantum[5] models.

This paper examines the detailed behavior of a vibrating and rotating diatomic molecule in an intense laser field, and investigates the validity of classical mechanics to describe this problem. The classical and quantum equations of motion are solved numerically for both rotating and, for comparison,non-rotating models of HF, initially in its ground state. Laser intensities of 1.0 and 2.5 TW/cm^2 are used, with frequencies in the region of the fundamental transition. Energy absorption and transition probabilities are calculated as a function of pulse time, as well as the pulse averaged absorption. Most of the work is for maximum pulse lengths between 0.9 and 2.0 picoseconds (between $\sim$100 and $\sim$250 optical cycles), although it was necessary to integrate the quantum solutions near multiphoton resonances for much longer times. It is found that classical mechanics does not correctly describe the time behavior of the system. Furthermore, classical rotational state distributions are completely incorrect. Classical mechanics, however, does give the correct magnitude of pulse averaged energy absorption. In addition, classical mechanics correctly indicates the presence of increased multiphoton absorption for frequencies lower than the one-photon resonance, although, in agreement with Walker and Preston's non-rotating results,[3] specific resonance peaks are not resolved and only a small amount of multiphoton absorption is seen. The effect of laser phase, which is often neglected, is also studied and found to be only a small effect on the quantum results and little or no effect on the classical results.

II. Methods

A. Classical Mechanics

The Hamiltonian for a vibrating and rotating diatomic molecule, with reduced mass μ, in spherical coordinates r, θ and ϕ is

$$H_o = \frac{p_r^2}{2\mu} + \frac{1}{2\mu r^2} \left(p_\theta^2 + p_\phi^2/\sin^2\theta\right) + V(r) \quad , \qquad \text{II-1}$$

where p_r, p_θ and p_ϕ are momenta canonically conjugate to r, θ and ϕ, and V(r) is the Born-Oppenheimer potential function. A Morse function is used to approximate the potential. In the absence of external fields, there are three conserved quantities which are the vibrational action $N_v = -\frac{\hbar}{2} + \frac{1}{2\pi} \oint p_r dr$, the rotational angular momentum $J = \left(p_\theta^2 + \frac{p_\phi^2}{\sin^2\theta}\right)^{\frac{1}{2}}$, and the z projection of the angular momentum $M = p_\phi$. If an oscillating electric field of frequency ω, z polarization and phase δ is introduced, the Hamiltonian becomes

$$H = H_o - d(r) \cos\theta \, E_o \sin(\omega t + \delta) \quad , \qquad \text{II-2}$$

where d(r) is the molecular dipole function and E_o is the field strength, which is related to the intensity by[6] $E_o = (8\pi I/c)^{\frac{1}{2}}$. Eq. II-2 is valid in the limit of high photon density which is certainly true for the present study. For very low intensities, the classical formalism developed by Miller[7] could be used.

With the interaction present, the vibrational action N_v and rotational angular momentum J are no longer conserved. However, with the present choice of polarization, M is still conserved since H has no ϕ dependence. The complete classical solution involves specification of the appropriate initial conditions and solution of Hamilton's equations:

$$\left.\begin{aligned}
\dot{p}_r &= -\frac{\partial H}{\partial r} = \frac{1}{\mu r^3}\left(p_\theta^2 + p_\phi^2/\sin^2\theta\right) - \frac{\partial V}{\partial r} + \frac{\partial d}{\partial r}\cos\theta\, E_o \sin(\omega t + \delta) \\
\dot{p}_\theta &= -\frac{\partial H}{\partial \theta} = p_\phi^2/\mu r^2 \sin^3\theta - d(r)\sin\theta\, E_o \sin(\omega t + \delta) \\
\dot{r} &= \partial H/\partial p_r = p_r/\mu \\
\dot{\theta} &= \partial H/\partial p_\theta = p_\theta/\mu r^2
\end{aligned}\right\} \quad \text{II-3}$$

Approximate analytic orbits have been obtained[8] for a rotating Morse oscillator with no external field, and these are used to determine diatomic initial conditions (see Appendix A for details). This approximation is excellent for the vibration-rotation levels of importance here. The laser phase δ is also averaged over in most cases (i.e., each trajectory has δ chosen randomly between 0 and 2π), although it will be shown to be unimportant.

The energy absorbed as a function of pulse length is defined by

$$\langle E(t)\rangle_{CL} = \frac{1}{N}\sum_{i=1}^{N} H_o(p_r^i(0), p_\theta^i(0), r^i(0), \theta^i(0), \delta^i; t) - E_1 \qquad \text{II-4}$$

where N is the number of trajectories and E_1 is the initial molecular energy, which in the present study is the ground state (v = 0, j = 0) energy. The final vibrational action N_v after a pulse of length t is also calculated with the rotating Morse oscillator[8] approximation. Appendix A shows that this is an excellent approximation for the states of interest here. J is calculated directly from $J(J+1)\hbar^2 = p_\theta^2 + p_\phi^2/\sin^2\theta$. (Note: $p_\phi = 0$ in the present study since J=0 initially.) With $\hbar$=1, N_v and J are boxed according to the nearest integers v,j such that $v-1/2 \leq N_v < v+1/2$ and $j-1/2 \leq J < j+1/2$, which is the usual quasiclassical quantization procedure. The transition probability into a particular v,j state, as a function of pulse length is

$$P_{v,j}^{CL}(t) = N_{v,j}(t)/N \qquad \text{II-5}$$

where $N_{vj}(t)$ is the number of trajectories with final actions in the v,j box.

Of course, a single trajectory integrated out to some large pulse length T contributes to all intermediate pulse time results. Similiar to Walker and Preston,[3] the pulse averaged energy as a function of laser frequency ω is defined as

$$\bar{E}_{Cl}(\omega) = \frac{1}{T}\int_0^T \langle E(t)\rangle_{CL}\, dt \quad . \qquad \text{II-6}$$

For comparison, non-rotating calculations were also performed. These calculations were done in the same manner as described by Walker and Preston.[3]

For technical details of the numerical calculations, see sec. II-C.

B. Quantum Mechanics

Although Leasure, Milfeld and Wyatt[5] have developed an efficient and elegant means of determining the long time solution, the time scale of interest here is short enough ($\lesssim$ 20ps) that direct integration of the coupled quantum equations is possible.

The total wave function is expanded as

$$\Psi_m(r,\theta,\phi,t) = \Sigma_{v,j} C_{vjm}(t)\chi_{vjm}(r,\theta,\phi) \qquad \text{II-7}$$

with

$$\chi_{vjm}(r,\theta,\phi) = R_v(r)\, Y_{jm}(\theta,\phi)/r \quad .$$

The Y_{jm} are spherical harmonics and R_v are Morse eigenfunctions.[9] Strictly speaking, R_v should also depend on j, but in the present problem, with only small values of j being important, such rotational corrections should be

small. As in classical mechanics, the z component of the angular momentum ($m\hbar$) is conserved. Since the present study involves j=0 initially, m is zero throughout. In all subsequent equations m is understood to be zero. If the molecule had $j \neq 0$ initially, it would be necessary to average over transition probabilities for all integer values of m such that $-j \leq m \leq j$.

Inserting eq. II-7 into the time-dependent Schrödinger equation results in the coupled equations

$$i \hbar \dot{C}_{vj}(t) = E^{o}_{vj} C_{vj} + \Sigma_{v'j'} D_{v'j'vj} C_{v'j'} E_o \sin(\omega t + \delta) , \qquad \text{II-8}$$

where the E^{o}_{vj} are eigenvalues of $\hat{H}_o$ and the $D_{v'j'vj}$ are matrix elements

$$D_{v'j'vj} = - \int_0^\infty R_{v'} \, d(r) \, R_v dr \times \begin{cases} \left[\frac{(j+1)^2}{(2j+1)(2j+3)}\right]^{\frac{1}{2}}, & j' = j+1 \\ \left[\frac{j^2}{(2j-1)(2j+1)}\right]^{\frac{1}{2}}, & j' = j-1 \end{cases} . \qquad \text{II-9}$$

It will be shown later, as with the classical results, that the laser phase δ does not appreciably effect the results. For efficiency, the majority of the quantum calculations are made with a fixed δ of $\pi/2$. The coefficients C_{vj} of eq. II-8 must be complex. Thus, writing $C_{vj} = X_{vj} + i Y_{vj}$, one obtains the coupled real equations

$$\begin{aligned} -\hbar \dot{Y}_{vj} &= E^{o}_{vj} X_{vj} + \Sigma_{v'j'} D_{v'j'vj} X_{v'j'} E_o \sin(\omega t + \delta) \\ \hbar \dot{X}_{vj} &= E^{o}_{vj} Y_{vj} + \Sigma_{v'j'} D_{v'j'vj} Y_{v'j'} E_o \sin(\omega t + \delta) \end{aligned} \qquad \text{II-10}$$

For comparison with the classical results, we will also be interested in the transition probabilities

$$P^{QM}_{vj}(t) = | C_{vj}(t) |^2 , \qquad \text{II-11}$$

the energy absorption

$$\langle E(t)\rangle_{QM} = \Sigma_{vj} \; P_{vj}^{QM}(t) \; E_{vj}^{o} - E_1 \quad , \qquad \text{II-12}$$

where E_1, the initial energy is taken to be the ground state energy, and the pulse length averaged energy absorption,

$$E_{QM}(\omega) = \frac{1}{T} \int_0^T \langle E(t)\rangle_{QM} \, dt \quad . \qquad \text{II-13}$$

We also study the non-rotating case in a similiar fashion. One may obtain the non-rotating equations by omitting all factors that include j and m in eqs. II-7 - II-12.

For technical details of the numerical calculations, see sec. II-C.

C. Computational Details

A Morse potential, $V = D(1 - e^{-\alpha(r-r_e)})^2$, was used for HF, with parameters[3] $D = 0.22509$, $\alpha = 1.1741$, and $r_e = 1.7329$ a.u. Since relatively low v states are involved, a linear approximation to the dipole function is satisfactory, $d(r) = d_o + d_1(r-r_e)$ with[5c] $d_o = 0.716$ and $d_1 = 0.310$ a.u. (1 Debye = 0.39343 a.u.) Some work, in fact, was done with a quadratic form for d(r),[4c] and that did not significantly affect our results.

Laser intensities of 1.0 and 2.5 TW/cm^2 were used, which correspond to field strengths E_o of 0.005338 and 0.008440 a.u., respectively. (1 V/cm = 1.9447×10^{-10} a.u.) The matrix elements $D_{v'j'vj}$ of eq. II-9 were evaluated numerically although analytical forms do exist.[9] Some typical elements are $D_{1100} \simeq 0.022$, $D_{2211} \simeq 0.028$, and $D_{2011} \simeq 0.032$ a.u.

For the classical rotating HF calculations, 1000 trajectories with random initial conditions (see Appendix A) were run for most frequencies. Monte Carlo errors in the quantities of interest were between 10 and 15%. For the non-rotating calculations, 50 trajectories were run for each

frequency. In this case it is more efficient to increment the vibrational angle variable in a step-wise fashion between 0 and 2π than to pick it randomly. The classical equations of motion were integrated with a standard predictor-corrector algorithm[10] to either 0.9 or 1.5 ps. The trajectories were back-integrable to four significant figures in all variables. Integration of the classical equations of motion beyond about 1.5 ps is extremely difficult due to the accumulation of error. The integration of oscillatory nonlinear differential equations over long time periods is still a current problem in numerical analysis.[11]

By between 0.9 and 1.5 ps, the pulse averaged energy absorption, eq. II-6, appears to be converging, but has not yet fully converged. However, reasonable estimates of the converged $\bar{E}_{CL}(\omega)$ can be obtained, since $\langle E(t)\rangle_{CL}$ has either reasonably leveled off or oscillates with a small amplitude. Thus, either the approximate leveled off value or the average of the oscillations in $\langle E(t)\rangle_{CL}$ is taken to be $\bar{E}_{CL}(\omega)$.

The quantum equations of motion, eqs. II-10, were integrated with the same predictor-corrector algorithm used in the classical claculations. An adequate basis for HF with the intensities and time scale of interest consisted of the first five v and first five j states, i.e. a 25 term expansion. The non-rotating quantum solutions were obtained in an analogous fashion, using the first five vibrational states in the wavefunction expansion. The solutions were stable to the addition of more basis functions and probability was conserved to at least nine significant figures. Most of the quantum solutions were integrated to 2 ps, although when the laser frequency was near a multiphoton resonance, it was necessary to integrate to times in the 10-20 ps range. Interestingly, because the quantum equations are linear, it is possible to integrate 50 coupled quantum equations to times exceeding

20 ps, which is much longer than it is practical to integrate only four nonlinear classical equations.

The quantum pulse averaged energy absorption, eq. II-13, was obtained by numerical integration. $\bar{E}_{QM}(\omega)$ was found to converge within 15% with maximum pulse lengths of 2 ps, except near the two multiphoton resonances ($\bar{\nu} = \omega/2\pi c$ = 3937 and 3879 cm^{-1} for rotating and 3879 cm^{-1} for non-rotating HF) where maximum pulse lengths between 10 and 20 ps were required for convergence. Note that it was sometimes necessary to average over small oscillations that were apparent in $\bar{E}_{QM}$ as a function of pulse length T to obtain the best estimate.

To aid in the interpretation of the results, Table I gives the relevant E^{o}_{vj} levels for HF, calculated with the rotating Morse oscillator formula.[8]

III. Results and Discussion

A. Energy Absorption Spectra

The quantum and classical pulse time averaged energy absorption spectra are plotted in Fig. 1a for non-rotating and Fig. 1b for rotating HF, with laser intensity 1.0 TW/cm^2. The plot for non-rotating HF is similiar to plots of Walker and Preston[3] for higher intensities ($\geq$ 10 TW/cm^2). At 1.0 TW/cm^2, though, the quantum structure is more resolved. The major features are a narrow two-photon resonance at $\bar{\nu}$ = 3879 cm^{-1} (i.e., the v = 0 to v = 2 absorption), and a broad one-photon resonance at 3966 cm^{-1} (the v = 0 to v = 1 absorption). The classical spectrum shows just one very broad peak with a maximum at about $\bar{\nu} \simeq$ 3940 cm^{-1}. While the classical spectrum does not have any of the quantum structure, examination of the classical state distribution does show the presence of a small amount of two-photon absorption, as the frequency is lowered. Details of this will

be given later.

For rotating HF, the spectra (Fig. 1b) are qualitatively similiar to the non-rotating case. There are three peaks in the quantum spectrum: one broad peak near $\bar{\nu}$ = 4006 cm^{-1} (the (v,j) ≡ (0,0) → (1,1) one-photon resonance) with a full width at half maximum (FWHM) of ∿50 cm^{-1}, and two narrow peaks near $\bar{\nu}$ = 3937 cm^{-1} (the (0,0) → (2,2) two-photon resonance) and 3879 cm^{-1} (the (0,0) → (2,0) two-photon resonance), each with a FWHM of < 10 cm^{-1}. The classical spectrum has one very broad peak which peaks near the (0,0) → (1,0) resonance at $\tilde{\nu}$ = 3966 cm^{-1}. Overall, the classical solution for rotating HF gives a general idea of the absorption. As in the non-rotating case, the classical result predicts increased two-photon absorption for frequencies red-shifted from the one-photon resonance, as will be seen below in sec. IIIB.

In Fig. 2, the rotating HF average energy absorption for I = 2.5 TW/cm^2 is shown. Qualitatively, the quantum peaks become broader and overlap more than the 1.0 TW/cm^2 case. There appears to be a small power shifting of the resonance peaks, toward higher frequencies, but it has not been resolved (see ref. 5c for a discussion of power shifting). Classically, the absorption also broadens relative to 1.0 TW/cm^2 and the peak maximum appears to shift to lower frequencies, indicating more multiphoton absorption.

B. Transition Probabilities

In this section the approximate time averaged transition probabilities into various states are examined qualitatively to help show the relative amounts of one and two photon absorption. Looking at the classical results, it is clear that classical mechanics does not give the correct rotational state distribution. Classically, there are large probabilities for ending

in the (0,1) and (1,0) states, which correspond to high order processes in quantum mechanics. These transitions are not observed to any large extent in the quantum results. To get a meaningful comparison, only the probabilities for ending in a particular vibrational level will be considered, i.e., a sum is taken over rotational states within a vibrational level.

Table II shows the quantum and classical time averaged probabilities at various frequencies for rotating and non-rotating HF, with I = 1.0 TW/cm^2. Each peak of the quantum solution can be seen to be either a one or a two photon absorption, with both processes observed appreciably only where peaks overlap. At higher intensities the peaks will broaden and overlap more, but each peak will still correspond to a particular absorption. The classical results do indicate the presence of some two photon absorption as the frequency is decreased. But classically, there is a very gradual change which results in the very broad single peak in the spectrum (Fig. 1), rather than the abrupt changes in the quantum results.

To show some intensity effects, average probabilities for rotating HF at 2.5 TW/cm^2 are given in Table III. For this larger intensity, both classically and quantum mechanically, the excited states become more populated.

C. Time Behavior

The previous two sections were concerned with average quantities. In this section the energy absorption and transition probabilities as a function of time are examined. The quantum mechanical laser phase used in this section was fixed at $\pi/2$. The effect of laser phase is examined in the next section.

In Fig. 3, a comparison of classical and quantum energy absorption as

a function of time is given for non-rotating HF at $\bar{\nu}$ = 3966 cm^{-1} (the one photon v=0 to v=1 resonance). The quantum results show oscillations with a period of about 0.75 ps with no sign of damping out to 1.5 ps. As this frequency and intensity (1.0 TW/cm^2) the solution is well approximated by a two-level system (i.e., the Rabi model[12a]). In contrast, the classical result oscillates with a frequency of about 0.4 ps and a smaller amplitude. Also, it appears as though the oscillations may be damping.

Fig. 4 shows the classical and quantum time dependent energy absorption for rotating HF with $\bar{\nu}$ = 4006 cm^{-1} (one photon (0,0) → (1,1) resonance). The results are similiar to those in Fig. 3 for non-rotating HF. In this case, though, the classical result appears to level off even faster. The behavior of the quantum solution is again well approximated by the two level Rabi model.[12a] The quantum solution has been followed for up to 20 ps with no clear sign of damping.

The quantum result for the two-photon resonance at 3937 cm^{-1} ((0,0) → (2,2) resonance) is considerably different (Fig. 5) The complicated nature of the oscillations may be contrasted with the Rabi oscillations of Fig. 4. From Fig 5 it can be seen that the two-photon absorption is a long time process. The corresponding classical result (Fig. 6) also seems to show some aspects of the slower growth in absorption, although the solution is reasonably level by 0.9 ps.

In Figs. 7, 8 and 9, plots are shown for some transition probabilities as a function of time, again for I = 1.0 TW/cm^2. Here, the classical solution is actually broken up into rotational levels, so that the discrepancy with quantum mechanics can be seen. The results for $\bar{\nu}$ = 4006 cm^{-1} are given in Fig. 7. The quantum solutions for P_{01} and P_{10} are not shown since they are very small ($\lesssim 10^{-2}$). Qualitatively, the probabilities show the same

behavior as the energy absorption as a function of time, i.e., the classical solutions tend to level off more and the quantum solutions appear periodic. Note that in reality there are high frequency, small amplitude oscillations that are superimposed on the quantum probabilities. These oscillations have not been resolved in our graphs and thus give rise to some roughness, particularly near peak maxima.

The classical probabilities for rotating HF at $\bar{\nu}$ = 3937 cm^{-1} are shown in Fig. 8. It can be seen that the v = 2 state gets significantly populated, but the v = 1 state is also significantly populated. The quantum probabilities near the two photon resonance at $\bar{\nu}$ = 3937 cm^{-1} are shown in Fig. 9. The resonant probability $P_{22}(t)$ displays a long period which essentially matches the period of $\langle E(t) \rangle_{QM}$ in Fig. 5. Another reasonably significant probability is P_{11}, which is not shown. $P_{11}(t)$ displays a higher frequency oscillation and can reach a maximum of $\sim$ 0.13. The other two-photon resonance, at $\bar{\nu}$ = 3879 cm^{-1}, is not plotted here. Qualitatively, the classical results for this frequency show much less excitation than for 3937 cm^{-1}. There is a small amount of v = 1 excitation and no v = 2 excitation. Essentially no rotational excitation is seen in the classical results for this frequency. The quantum results for 3879 cm^{-1} show somewhat less excitation into the (1,1) state than for 3937 cm^{-1}, and again the resonant probability, P_{20}, displays a long period.

D. Laser Phase Effect

Based on the classical and quantum equations of motion (eqs. II-3 and II-8), without additional approximations, one would expect the solution to be dependent on the choice of laser phase δ. Without allowing for the details of how the field is turned on, a complete study should involve

averaging over the laser phase to obtain the most meaningful results.[13]

The laser phase dependence, however, disappears from the quantum equations in the rotating wave approximation,[12] as shown in Appendix B for the two state model. However, for sufficiently large field strengths or de-tuning of ω from resonance, the rotating wave approximation will breakdown.[12c] Thus, for example, Moloney and Meath[13] have shown the laser phase dependence of probabilities as a function of time for a two state model. They found increasing phase effects for larger field strengths and at multiphoton resonances.

The situation is not quite as clear in the classical analysis. However, if only the relative difference between laser and vibrational phases is important, then it would be sufficient to average only over the vibrational phase, without averaging over the laser phase, i.e., the laser phase would not matter. The conditions for this to be true probably include that ω be close to resonance.

To access the effect of laser phase δ on the present problem, consider first non-rotating HF. For an intensity of 1.0 TW/cm^2 and frequencies of 3966 and 3879 cm^{-1}, the classical solutions were obtained for fixed δ of 0 and $\pi/2$. 500 trajectories were run for each solution to ensure no statistical error. Over the entire 1.5 ps range, $\langle E(t) \rangle_{CL}$ for the two phases agreed to between 2 and 4 significant figures. The quasiclassical probabilities also were in excellent agreement. Similarly, the non-rotating quantum results for the same conditions showed little phase dependence.

We also examined rotating HF at 1.0 TW/cm^2 for the possibility of phase effects. Within the Monte Carlo error ($\lesssim$ 15%), no clear phase effect can be distinguished in the classical results. However, slight discrepancies in the time-dependent quantum solutions may be seen, since no

statistical error is present. Table IV lists some relevant probabilities and $\langle E(t)\rangle_{QM}$ for $\delta = 0$ and $\pi/2$, at $\bar{\nu} = 4006\ cm^{-1}$. Other phases between 0 and π were also examined, but the largest differences were found between $\delta = 0$ and $\delta = \pi/2$. Despite $\bar{\nu}$ being almost exactly on resonance, slight differences may be noted, particularly in the probabilities. These differences become larger near peak maxima and can be as much as 4%. However, such differences are comparable in amplitude to the high frequency oscillations that are superimposed on the Rabi oscillations and do not appreciably effect the overall behavior. Notice that $\langle E(t)\rangle_{QM}$ is not effected much by these differences, indicating that the other probabilities, which are small and not listed, tend to compensate. Table V presents similar results for $\bar{\nu} = 3937\ cm^{-1}$. Although this is a two-photon resonance, the discrepancies due to laser phases are comparable to the $\omega = 4006\ cm^{-1}$ results. Thus, for intensities $\sim 1.0\ TW/cm^2$, and the present frequency range, the effect of laser phase is small and can be neglected for most practical purposes.

IV. Concluding Remarks

In summary, the detailed dynamics of both rotating and non-rotating models for HF in an intense laser has been investigated with both classical and quantum mechanics. The frequency range covered included one-photon as well as two-photon resonances.

It is found that classical mechanics does not predict the correct rotational state distributions. Also, the time behavior of the classical solution is qualitatively different from the quantum one. Classical mechanics does give the correct magnitude of pulse time averaged quantities such as the average energy absorption, but does not give the detailed resonance

peaks for multiphoton absorptions. Classical mechanics does correctly indicate more multiphoton absorption as the frequency is red-shifted from the one-photon resonance, but it predicts far too little such absorption.

The laser phase has clearly been shown to be an unimportant effect for the transitions and intensities of interest here, although it could conceivably be important for much higher intensities.

It is difficult to extend these conclusions to polyatomic systems in intense laser fields, which are of greater interest. These results do indicate, however, that care should be taken when classical mechanics is applied to molecular systems. There is the real possibility, of course, that the increased number of states in a polyatomic could make classical mechanics a better approximation to quantum mechanics than for the present case of a diatomic. The same may be true for a diatomic initially in an excited state, or in a more intense field, where more states may become populated.

Acknowledgments

We would like to thank Professor W. H. Miller for encouragement and for reviewing a preliminary version of this manuscript, and Professor R. E. Wyatt for several informative discussions and for showing us some of his unpublished results. We also thank Domenic Ali and Yitzhak Weissman for some instructive comments. Thanks are also due other members of our research group, Boyd Waite, Lynn Hubbard, Shenghua Shi, and Steven Schwartz. This work was supported by Director, Office of Energy Research, Office of Basic Energy Sciences, Chemical Sciences Division of the U.S. Department of Energy under Contract No. DE-AC03-76SF00098, and also in part by the National Science Foundation under grant CHE-79-20181. SKG gratefully acknowledges the Natural Sciences and Engineering Research Council of Canada for partial support.

Appendix A. Initial and final conditions for a diatomic molecule in the rotating Morse oscillator approximation.

To clasically determine probabilities, it is necessary to average over initial conditions. For an isolated diatomic molecule, one can change variables to action-angle variables (N_v, Q_v), (J, Q_J) and (M, Q_M) such that $\dot{N}_v = \dot{J} = \dot{M} = 0$, with N_v being the vibrational action, J the rotational action or angular momentum and M being the projection of the angular momentum onto the z axis. These variables allow a connection with quantum mechanical states to be made easily.[8] The probability P of some event may be obtained by averaging over the initial angle variables Q_v, Q_J, Q_M for fixed N_v, J and M,

$$P = (2\pi)^{-3} \int_0^{2\pi} dQ_v \int_0^{2\pi} dQ_J \int_0^{2\pi} dQ_M \, \chi_{N_v\, J\, M}(Q_v, Q_J, Q_M) \qquad \text{A-1}$$

where $\chi = 1$ if the event occurs and 0 if it doesn't occur for the given initial conditions. Usually, the angular momentum is randomly oriented in space, so an average may be taken over M:

$$\overline{P} = \int_{-J}^{J} dM \, P \Big/ \int_{-J}^{J} dM = \frac{1}{2J} \int_{-J}^{J} dM \, P \qquad \text{A-2}$$

To do the Monte Carlo integration,[14] the variables of integration are changed to $\vec{\xi}$, with $0 \leq \xi_i \leq 1$, such that

$$\begin{aligned} 2\,\xi_1 - 1 &= M/J = \lambda \\ 2\pi\,\xi_2 &= Q_v \\ 2\pi\,\xi_3 &= Q_J \\ 2\pi\,\xi_4 &= Q_M \end{aligned} \qquad \text{A-3}$$

Eq. A-2 then becomes

$$\overline{P} = \lim_{N \to \infty} \frac{1}{N} \sum_{\vec{\xi}}^{N} \chi_{N_v\ J\ M}(\vec{\xi}) \qquad \text{A-4}$$

That is, one averages χ over N random evaluations of $\vec{\xi}$ (each component of $\vec{\xi}$ is taken to be a pseudo-random number for a given evaluation).

Approximate relations between the action-angle variables and ordinary molecular coordinates have been given by Porter, Raff and Miller[8] for a rotating Morse oscillator. The orbits given by them for θ and ϕ are not strictly correct. The corrected orbits are

$$r(t) = r_e - \frac{1}{\alpha} \ell n \{(-2a)[b + \sqrt{b^2 - 4ac}\ \sin(\omega_N t + Q_N)]\} \qquad \text{A-5a}$$

$$\theta(t) = \arccos [\sqrt{1 - \lambda^2}\ \cos(\omega_J t + Q_J + \text{sign}(p_r)\ J\Delta_J)] \qquad \text{A-5b}$$

$$\phi(t) = Q_M + \text{sign}(p_\theta) \arccos\left(\frac{\lambda \cot[\theta(t)]}{\sqrt{1 - \lambda^2}}\right) \qquad \text{A-5c}$$

where the formulae for a, b, c, w_N, ω_J and Δ_J may be found in Ref. 8 and are not repeated here. The errors in the angular orbits arose from omission of a sign (p_r) and sign (p_θ) factor in the generators W_r and W_θ respectively (eqs. 8a and 8b of ref. 8). Another slight error is in eqs. 30b and 30c of ref. 8. Here, the factor r^2 should be replaced by the expansion for r^2 given by their eq. 3.

Thus, to generate the initial conditions for a diatomic we first pick λ, Q_v, Q_J, and Q_M randomly according to eqs. A-3. Then, since the calculations are to be made in spherical coordinates, r, θ and ϕ are calculated from eqs. A-5. p_r and p_θ may be obtained by either conservation of energy and angular momentum, or by differentiation of eqs. 30 of ref. 8. This procedure is completely equivalent to randomly orienting the molecule and its angular momentum vector and picking

only r and p_r from the action-angle variable formulae, which is the more standard approach.[14] Thus the present approach offers no technical advantage over the ordinary approach for most applications, including the present one, except when the rotational angle variables play an important role, as in some semiclassical applications.

The vibrational action N_v is calculated at a time t from the approximate formula of ref. 8,

$$N_v = -\frac{\hbar}{2} + \frac{\sqrt{2\mu}}{\alpha}\left(\frac{b}{2\sqrt{-c}} - \sqrt{-a}\right) \qquad \text{A-6}$$

and only depends on the molecular energy and angular momentum state $J(J+1)\hbar^2 = (P_\theta^2 + P_\phi^2/\sin^2\theta)$. N_v was calculated numerically ($N_v = -\frac{\hbar}{2} + \frac{1}{2\pi}\oint p_r dr$) as a check on eq. A-6 and, for all N_v and J with $J \lesssim 10$, N_v from eq. A-6 is accurate to three significant figures. Thus, essentially no error is introduced by the use of eq. A-6 for N_v in the present study.

Appendix B. Effect of laser phase on the two state model.

For a two state model with states labeled A and B, eqs. II-8 become ($\hbar$=1)

$$\left.\begin{aligned} i\,\dot{C}_A &= C_A E_A^{\,o} + C_B D_{AB} E_o \sin(\omega t + \delta) + C_A D_{AA} E_o \sin(\omega t + \delta) \\ i\,\dot{C}_B &= C_B E_B^{\,o} + C_A D_{AB} E_o \sin(\omega t + \delta) + C_B D_{BB} E_o \sin(\omega t + \delta) \end{aligned}\right\} \quad \text{B-1}$$

If one now replaces C_A and C_B by S_A and S_B such that

$$\begin{aligned} C_A &= S_A\, e^{-iE_A^{\,o}t} \\ C_B &= S_B\, e^{-iE_B^{\,o}t} \end{aligned} \quad \text{B-2}$$

one obtains ($E_{AB} \equiv E_A^{\,o} - E_B^{\,o}$)

$$\begin{aligned} \dot{S}_A &= \tfrac{1}{2}\{S_B D_{AB} E_o [e^{-i(E_{AB}+\omega)t} e^{-i\delta} - e^{-i(E_{AB}-\omega)t} e^{i\delta}] + S_A E_o D_{AA} [e^{-i(\omega t+\delta)} - e^{i(\omega t+\delta)}]\} \\ \dot{S}_B &= \tfrac{1}{2}\{S_A D_{AB} E_o [e^{i(E_{AB}-\omega)t} e^{-i\delta} - e^{i(E_{AB}+\omega)t} e^{i\delta}] + S_B E_o D_{BB} [e^{-i(\omega t+\delta)} - e^{i(\omega t+\delta)}]\} \end{aligned} \quad \text{B-3}$$

The rotating wave approximation[12] involves omitting the highly oscillatory terms involving $e^{\pm i(E_{AB}+\omega)t}$ and $e^{\pm i\omega t}$. Thus

$$\begin{aligned} \dot{S}_A &= -\tfrac{1}{2} S_B D_{AB} E_o\, e^{-i(E_{AB} - \omega)t} e^{i\delta} \\ \dot{S}_B &= \tfrac{1}{2} S_A D_{AB} E_o\, e^{i(E_{AB} - \omega)t} e^{-i\delta} \end{aligned} \quad \text{B-4}$$

Within this approximation, it can easily be shown that the effect of laser phase δ is not important. To see this, the substitution $S_B' = S_B e^{i\delta}$ is made, so that B-4 becomes

$$\begin{aligned} \dot{S}_A &= -\tfrac{1}{2} S_B' D_{AB} E_o\, e^{-i(E_{AB} - \omega)t} \\ \dot{S}_B' &= \tfrac{1}{2} S_A D_{AB} E_o\, e^{i(E_{AB} - \omega)t} \end{aligned} \quad \text{B-5}$$

i.e., S_A and S_B' may be obtained by solving B-5 and the probabilities $P_A = |S_A|^2$ and $P_B = |S_B|^2 = |S_B'|^2$ have no phase dependence. Alternatively, eq. B-4 can be expressed as a second order equation in which the radiation phase does not appear.

One should note carefully that the rotating wave approximation is valid only if[12c] (i) $\omega \approx E_{AB}$ and (ii) $\omega >> D_{AB}E_o, D_{AA}E_o, D_{BB}E_o$. The second condition is often not stated, but is necessary if the oscillatory terms are to be unimportant. Consider, for example, HF in a 1.0 TW/cm^2 laser near the one-photon resonance at 4006 cm^{-1} with state A = (0,0) and B = (1,1). Condition (i) is satisfied and, with E_o = 0.00534 a.u., $D_{AB} \simeq 0.022$ a.u., $D_{AA} \approx D_{BB} \approx 0$, condition (ii) is 0.0182 >> 0.0001, which is reasonably satisfied.

References

1. See, for example, papers in "Advances in Laser Chemistry", ed. by A. H. Zewail, (Springer, N.Y., 1978) and "Laser-Induced Processes in Molecules", ed. by K. L. Kompa and S. D. Smith, (Springer, N.Y., 1978).
2. (a) D. Poppe, Chem Phys. 45, 371 (1980).
   (b) D. W. Noid, M. L. Koszykowski, R. A. Marcus and J. D. MacDonald, Chem. Phys. Lett. 51, 540 (1977).
   (c) D. W. Noid, C. Bottcher and M. L. Koszykowski, Chem. Phys. Lett. 72, 397 (1980). Note this last reference contains a classical-quantum comparison for a model non-rotating bent triatomic.
3. R. B. Walker and R. K. Preston, J. Chem. Phys. 67, 2017 (1977).
4. (a) D. W. Noid and J. R. Stine, Chem. Phys. Lett. 65, 153 (1979).
   (b) J. R. Stine and D. W. Noid, Chem. Phys. Lett. 77, 287 (1981).
   (c) K. M. Christoffel and J. M. Bowman, J. Chem. Phys. 85, 2159 (1981).
5. (a) S. C. Leasure and R. E. Wyatt, Opt. Eng. 19, 46 (1980).
   (b) S. C. Leasure and R. E. Wyatt, Chem. Phys. Lett. 61, 625 (1979).
   (c) S. C. Leasure, K. F. Milfeld and R. E. Wyatt, J. Chem. Phys. 74, 6197 (1981).
6. W. H. Flygare, "Molecular Structure and Dynamics", (Prentice-Hall, Englewood Cliffs, N.J., 1978) p. 11.
7. W. H. Miller, J. Chem. Phys. 69, 2188 (1978).
8. R. N. Porter, L. M. Raff and W. H. Miller, J. Chem. Phys. 63, 2214 (1975). Note our Appendix A gives some corrections to this paper.
9. (a) M. L. Sage, Chem. Phys. 35, 375 (1978).
   (b) R. Wallace, Chem. Phys. Lett. 37, 115 (1976).

10. L. F. Shampine and M. K. Gordon, "Computer Solution of Ordinary Differential Equations: The Initial Value Problem", (Freeman, S.F., 1975). The actual program used was ODE from the SANDIA Laboratory.

11. C. W. Gear, SIAM Review, 23, 10 (1981).

12. (a) M. Sargent, M. O. Scully, and W. E. Lamb, "Laser Physics", (Addison-Wesley, Reading, MA, 1974).

(b) S. Flugge, "Practical Quantum Mechanics", (Springer, N.Y., 1971), Vol. II, p. 138.

(c) M. Quack, J. Chem. Phys. 69, 1282 (1978).

13. J. V. Moloney and W. J. Meath, Mol. Phys. 31, 1537 (1976).

14. R. N. Porter and L. M. Raff, in "Modern Theoretical Chemistry", Vol. 2, Part B, W. H. Miller, editor (Plenum, N.Y., 1976), pp. 1-52.

Table I. Relevant energy levels for HF, according to the rotating Morse oscillator approximation.

v	j	$E^{o}_{v\,j}$ a.u.	$E^{o}_{v\,j}$ cm^{-1}
0	0	0.0093309	2048
0	1	0.0095187	2089
0	2	0.0098941	2171
1	0	0.0274001	6014
1	1	0.0275819	6054
1	2	0.0279454	6133
2	0	0.0446793	9806
2	1	0.0448551	9845
2	2	0.0452065	9922

Table II. Approximate time averaged probabilities for vibrational transitions of HF in a 1.0 TW/cm^2 laser.

	non-rotating			rotating		
$\bar{\nu}(cm^{-1})$	P_0	P_1	P_2	P_0	P_1	P_2
3850	0.88(QM)	0.08	0.04	0.99	0.01	0.00
	1.00(CL)	0.00	0.00			
3879	0.47	0.08	0.45	0.53	0.03	0.44
	0.88	0.12	0.00	0.99	0.01	0.00
3900	0.83	0.11	0.06	0.96	0.03	0.01
	0.73	0.19	0.08	0.94	0.04	0.02
3937	0.69	0.28	0.03	0.47	0.07	0.46
	0.69	0.24	0.06	0.67	0.27	0.06
3966	0.51	0.47	0.02	0.87	0.12	0.01
	0.63	0.36	0.01	0.58	0.40	0.02
4006	0.69	0.30	0.01	0.50	0.49	0.01
	0.68	0.32	0.00	0.66	0.34	0.00
4085	0.93	0.07	0.00	0.95	0.05	0.00
	0.90	0.10	0.00	0.88	0.12	0.00

Table III. Approximate time averaged vibrational transition probabilities for rotating HF in a 2.5 TW/cm^2 laser.[a]

$\bar{\nu}(cm^{-1})$	P_0	P_1	P_2
3879	0.51(QM)	0.07	0.42
	0.88(CL)	0.07	0.05
3900	0.90	0.05	0.05
	0.67	0.17	0.16
3937	0.48	0.10	0.42
	0.50	0.31	0.19
3966	0.77	0.18	0.05
	0.52	0.39	0.09
4006	0.52	0.45	0.03
	0.61	0.37	0.02
4085	0.89	0.11	0.00
	0.78	0.20	0.00

(a) The classical results shown for $\bar{\nu}$ = 3879 and 3937 cm^{-1} were actually run at 3870 and 3927 cm^{-1}, respectively. The probabilities will not vary much since the classical peak is broad. It was displayed in the table this way to avoid confusion since the overall trends are still clear.

Table IV. Quantum mechanical transition probabilities and energy absorbed as a function of pulse time for laser phases of 0 and $\pi/2$ at $\omega = 4006\ cm^{-1}$ and $I = 1.0\ TW/cm^2$.

	P_{00}		P_{22}		$E(t)_{QM}$(a.u.)	
t(ps)	$\delta = 0$	$\delta = \pi/2$	$\delta = 0$	$\delta = \pi/2$	$\delta = 0$	$\delta = \pi/2$
0.0	1.00	1.00	0.00	0.00	0.0000	0.0000
0.4	0.30	0.32	0.63	0.66	0.0125	0.0126
0.8	0.13	0.14	0.81	0.83	0.0156	0.0158
1.2	0.94	0.95	0.05	0.05	0.0010	0.0009
1.6	0.51	0.53	0.44	0.45	0.0084	0.0086
2.0	0.03	0.03	0.92	0.92	0.0177	0.0179
2.4	0.81	0.81	0.17	0.17	0.0034	0.0033
2.8	0.73	0.73	0.24	0.24	0.0047	0.0048
3.2	0.01	0.01	0.95	0.94	0.0180	0.0182
3.6	0.62	0.62	0.36	0.36	0.0068	0.0069
4.0	0.88	0.90	0.09	0.09	0.0018	0.0017
4.4	0.08	0.09	0.87	0.88	0.0167	0.0169

Table V. Quantum mechanical transition probabilities and energy absorbed as a function of pulse times for laser phases of 0 and $\pi/2$ at $\omega = 3937\ cm^{-1}$ and $I = 1.0\ TW/cm^2$.

	P_{00}		P_{22}		$\langle E(t)\rangle_{QM}$ (a.u.)	
t(ps)	$\delta = 0$	$\delta = \pi/2$	$\delta = 0$	$\delta = \pi/2$	$\delta = 0$	$\delta = \pi/2$
0.0	1.00	1.00	0.00	0.00	0.0000	0.0000
0.4	0.93	0.93	0.05	0.05	0.0021	0.0019
0.8	0.78	0.80	0.19	0.19	0.0072	0.0071
1.2	0.57	0.58	0.37	0.38	0.0142	0.0144
1.6	0.36	0.37	0.57	0.57	0.0218	0.0219
2.0	0.18	0.18	0.71	0.74	0.0282	0.0284
2.4	0.05	0.05	0.83	0.81	0.0320	0.0324
2.8	0.00	0.00	0.83	0.86	0.0333	0.0338
3.2	0.03	0.03	0.80	0.80	0.0322	0.0324
3.6	0.14	0.13	0.69	0.71	0.0283	0.0287
4.0	0.27	0.29	0.56	0.57	0.0231	0.0233
4.4	0.47	0.47	0.40	0.40	0.0169	0.0170

Figure Captions

Figure 1. Classical and quantum mechanical time averaged energy absorption for HF in a 1.0 TW/cm^2 laser. a) non-rotating HF, b) rotating HF.

Figure 2. Classical and quantum mechanical time averaged energy absorption for rotating HF in a 2.5 TW/cm^2 laser.

Figure 3. Time-dependent energy absorption for non-rotating HF with $\bar{\nu}$ = 3966 cm^{-1} and I = 1.0 TW/cm^2.

Figure 4. Time-dependent energy absorption for rotating HF with $\bar{\nu}$ = 4006 cm^{-1} and I = 1.0 TW/cm^2.

Figure 5. Quantum mechanical time-dependent energy absorption for rotating HF with $\bar{\nu}$ = 3937 cm^{-1} and I = 1.0 TW/cm^2. Note that the jaggedness is due to poor resolution of the high frequency oscillations.

Figure 6. Classical time-dependent energy absorption for rotating HF with $\bar{\nu}$ = 3937 cm^{-1} and I = 1.0 TW/cm^2.

Figure 7. Classical and quantum mechanical probabilities P_{vj} for HF with $\bar{\nu}$ = 4006 cm^{-1} and I = 1.0 TW/cm^2. The jaggedness of the quantum results is due to poor resolution of the high frequency oscillations.

Figure 8. Classical probabilities P_{vj} for HF with $\bar{\nu}$ = 3937 cm^{-1} and I = 1.0 TW/cm^2.

Figure 9. Quantum mechanical probabilities P_{00} and P_{22} for HF with $\bar{\nu}$ = 3937 cm^{-1} and I = 1.0 TW/cm^2. The jaggedness is due to poor resolution of the high frequency oscillations.

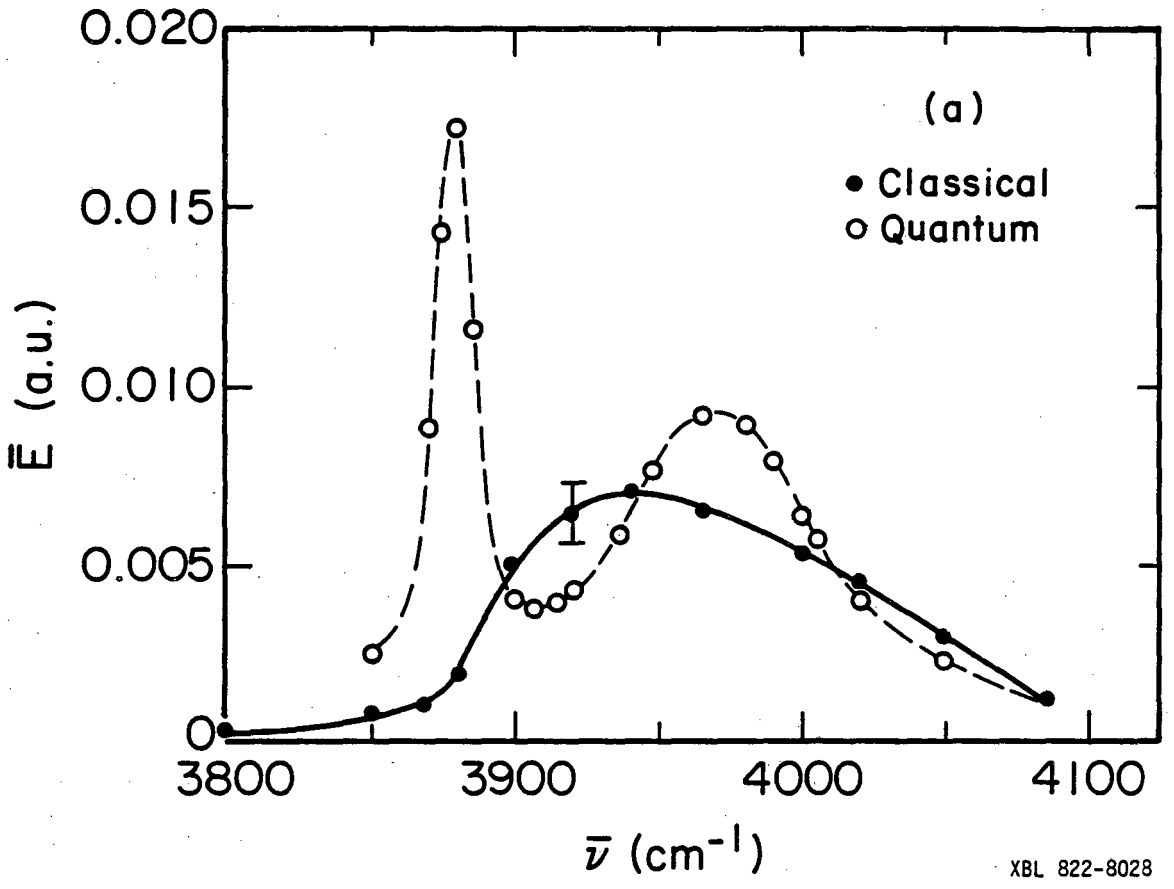
0.020
0.015
0.010
0.005
0
3800
3900
4000
4100
(a)
• Classical
o Quantum
$\bar{E}$ (a.u.)
$\bar{\nu}$ (cm^{-1})
XBL 822-8028

Figure 1a

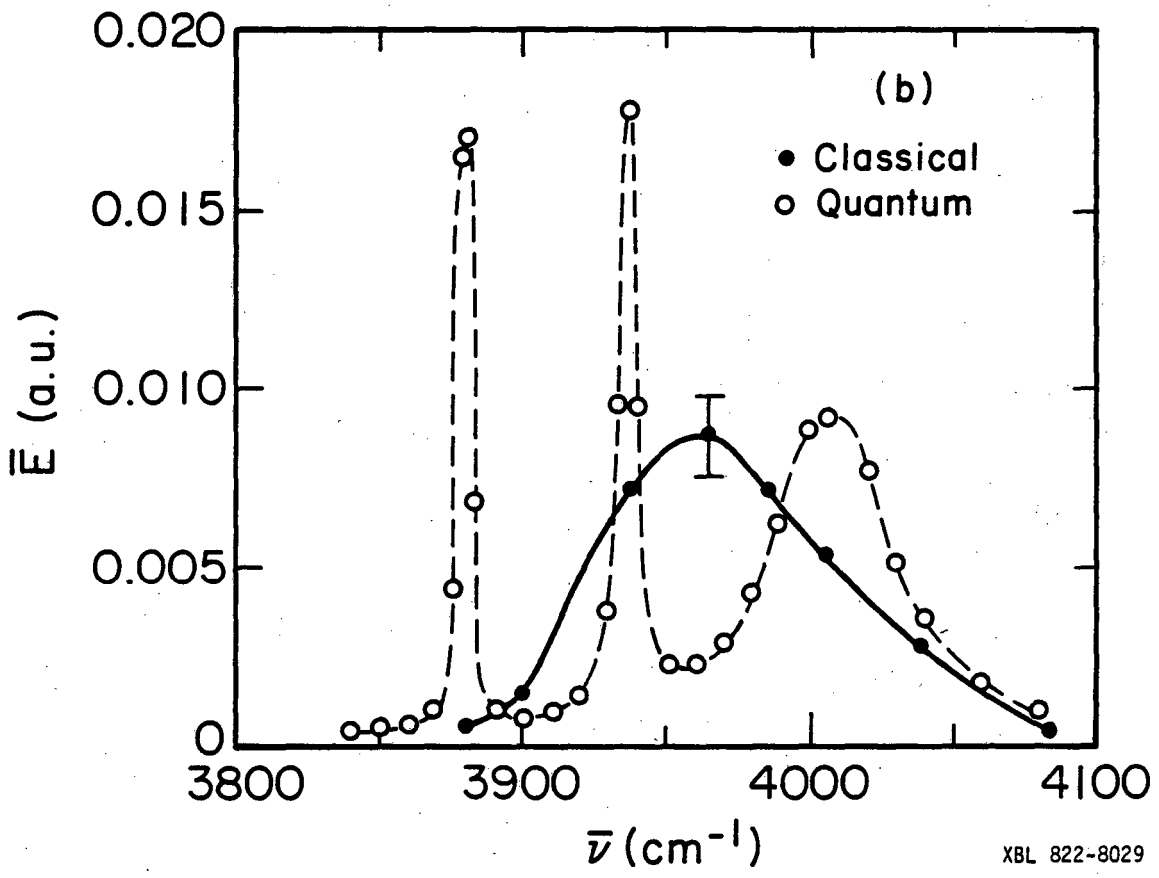
0.020
0.015
0.010
0.005
0
$\bar{E}$ (a.u.)
(b)
• Classical
o Quantum
3800
3900
4000
4100
$\bar{\nu}$ (cm^{-1})
XBL 822-8029

Figure 1b

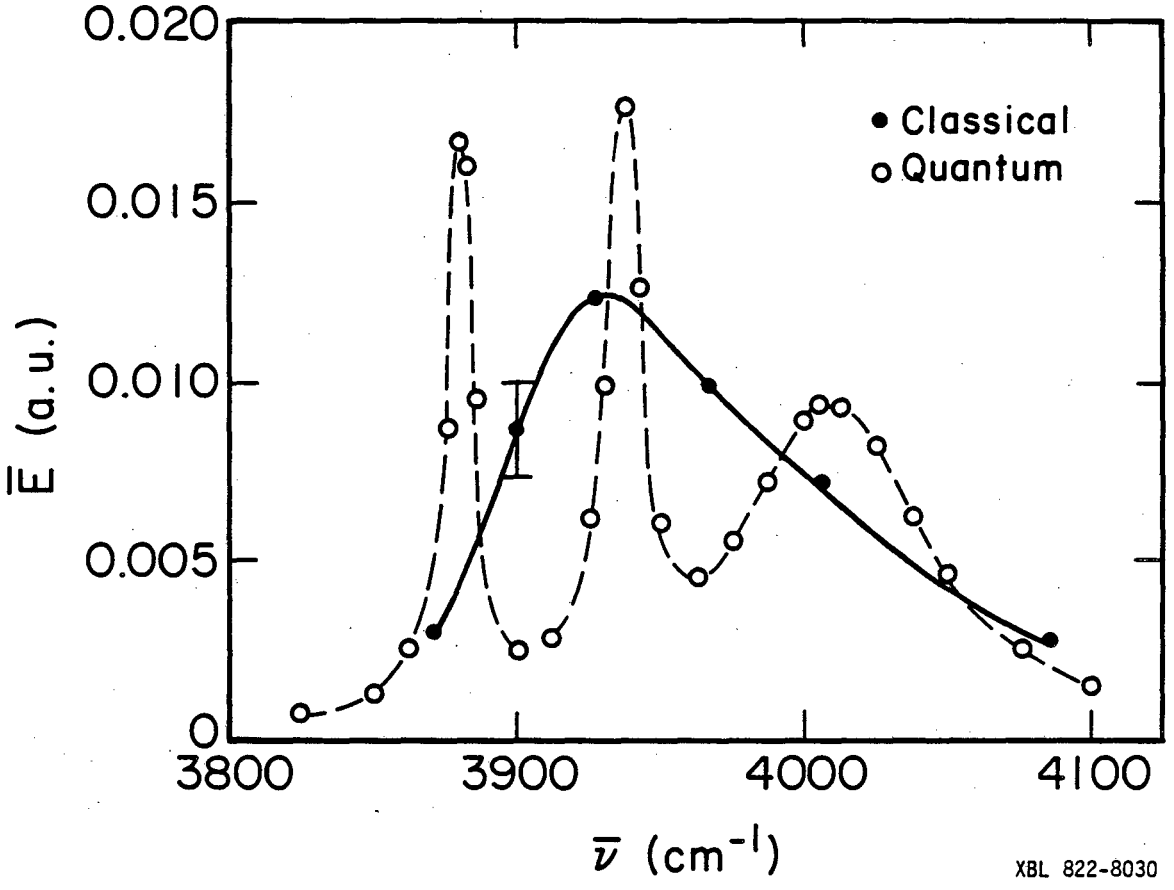
0.020
0.015
0.010
0.005
0
3800
3900
4000
4100
$\bar{E}$ (a.u.)
$\bar{\nu}$ (cm^{-1})
• Classical
o Quantum
XBL 822-8030

Figure 2

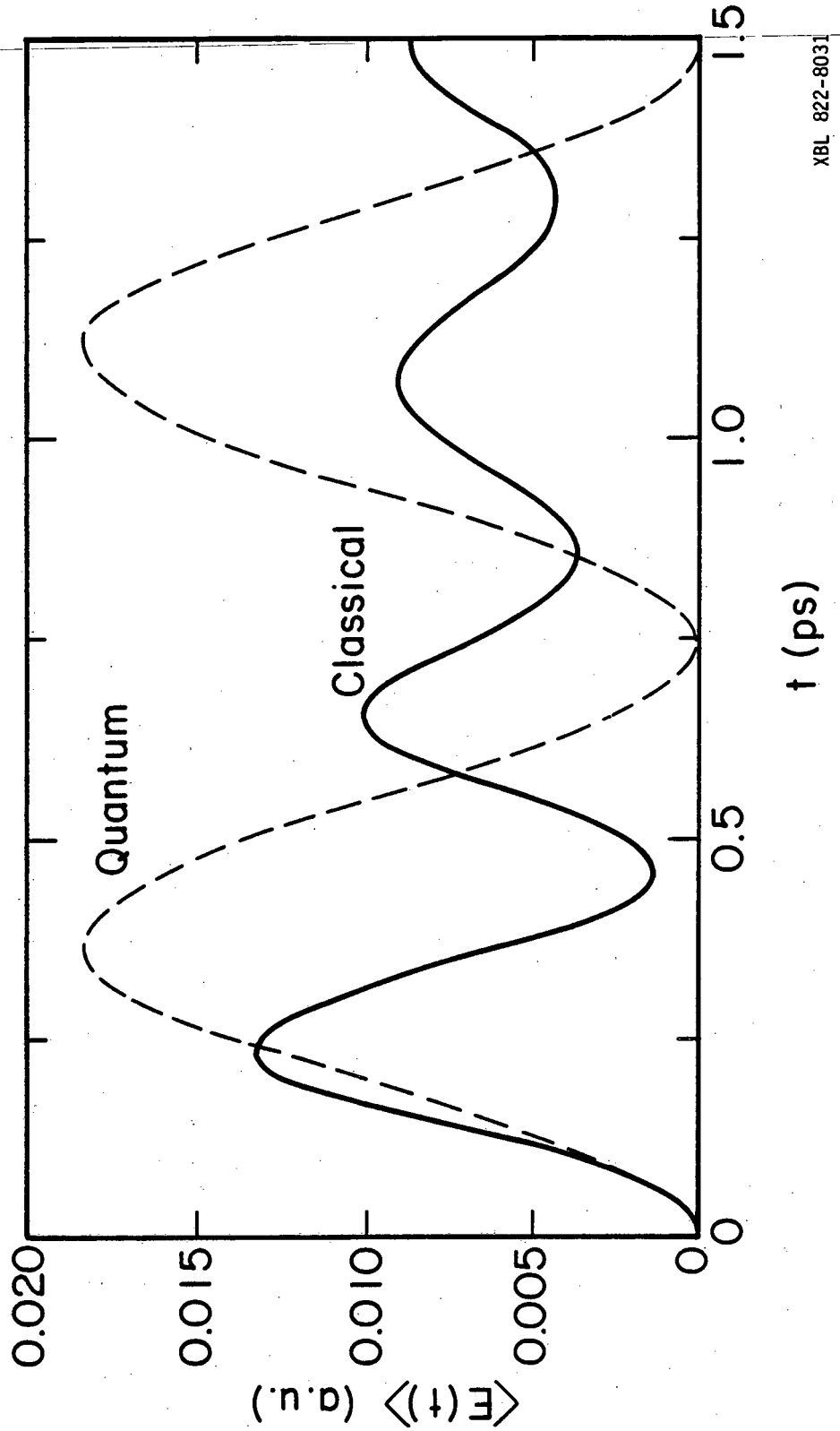
Quantum
Classical
0.020
0.015
0.010
0.005
0
0
0.5
1.0
1.5
t (ps)
⟨E(t)⟩ (a.u.)
XBL 822-8031

Figure 3

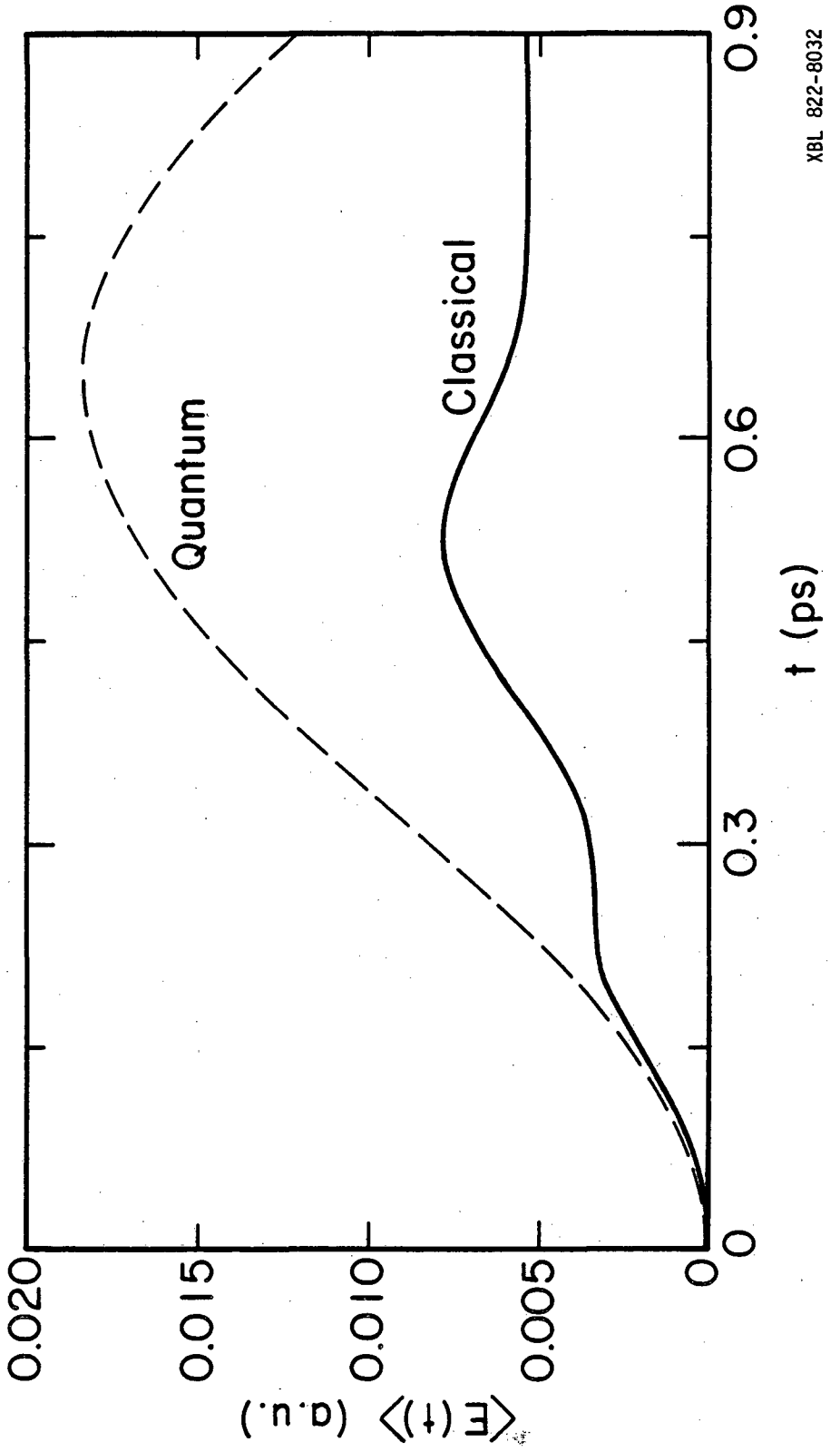
Quantum
Classical
0.020
0.015
0.010
0.005
0
0.3
0.6
0.9
t (ps)
⟨E(t)⟩ (a.u.)
XBL 822-8032

Figure 4

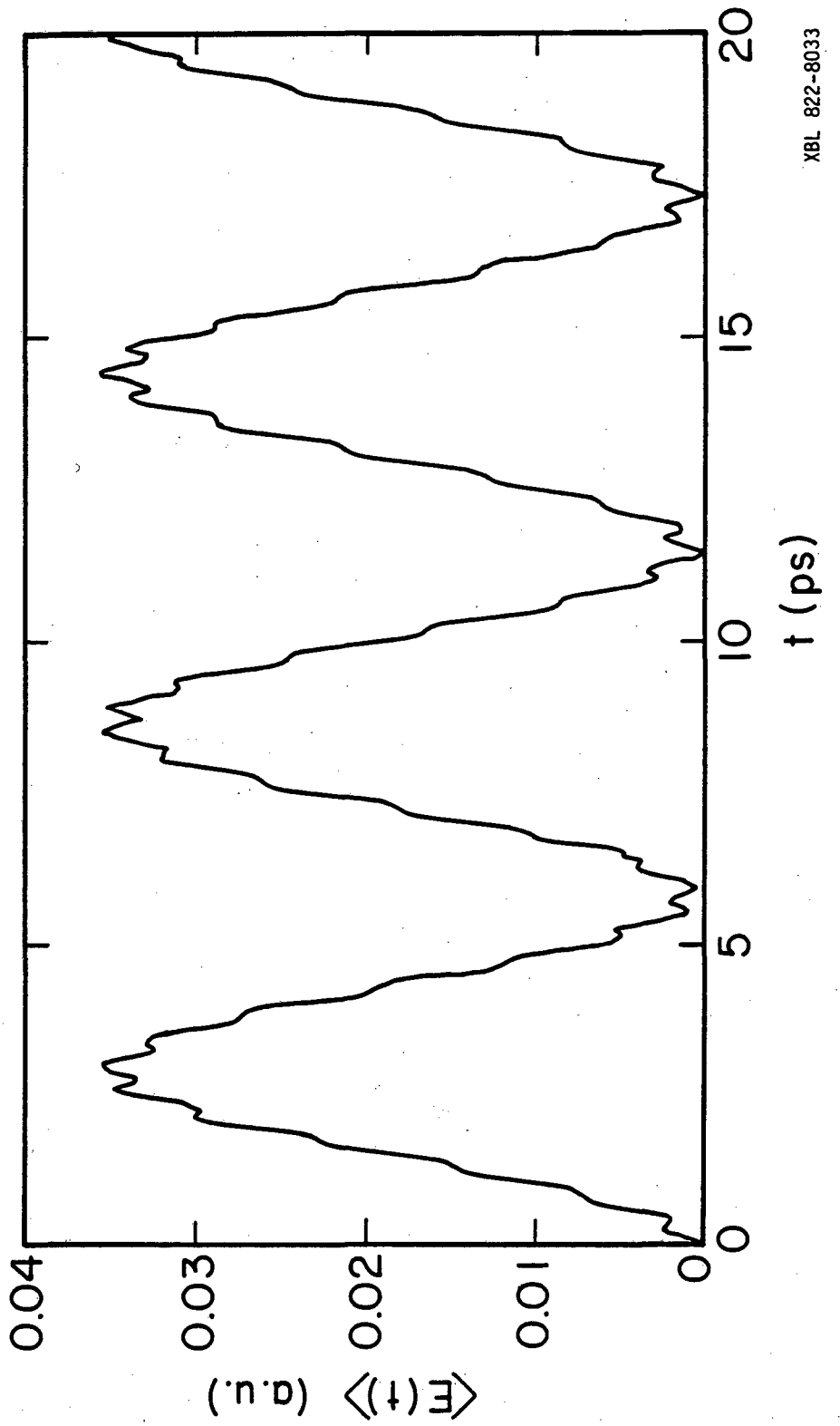

Figure 5

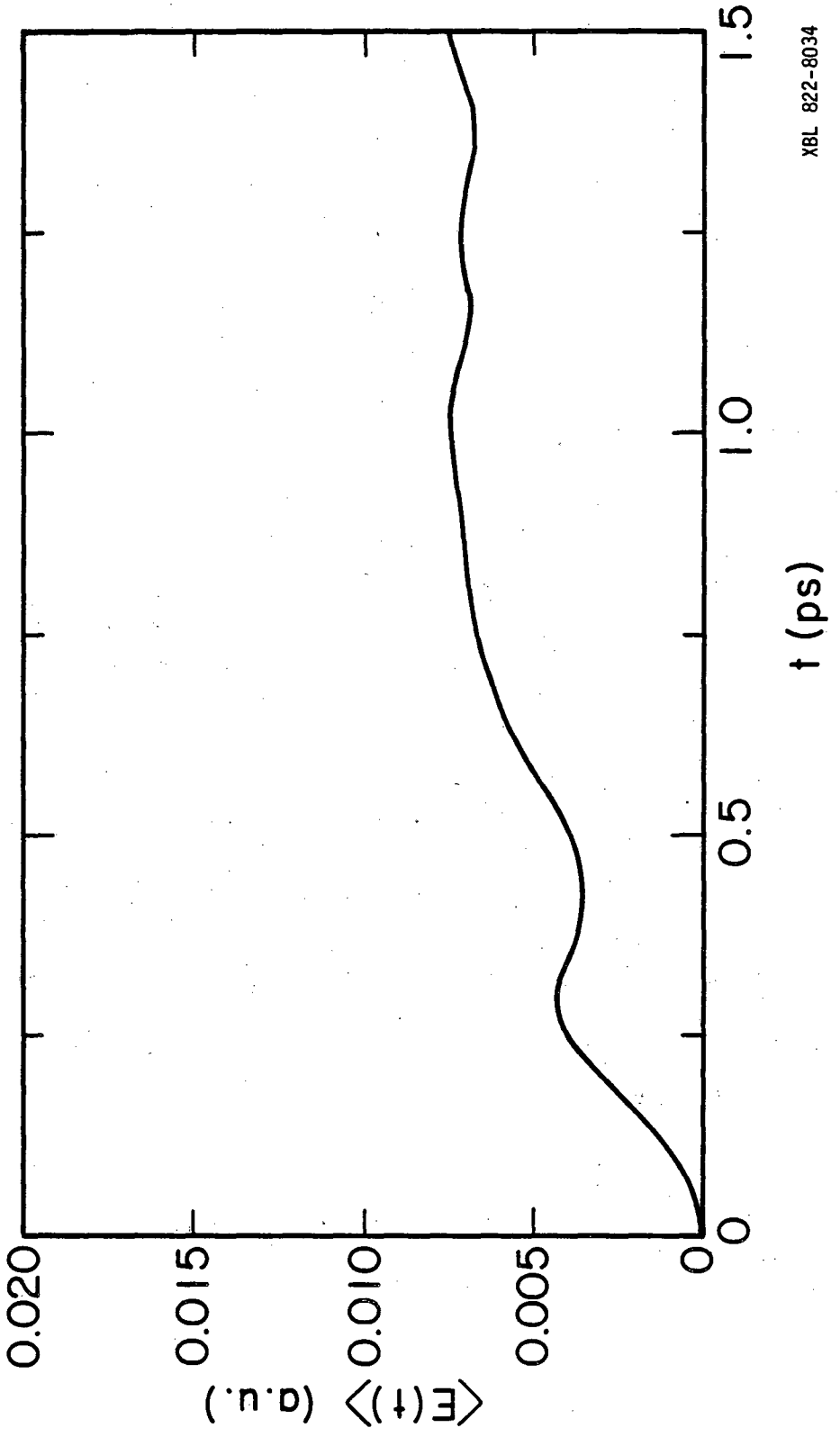

Figure 6

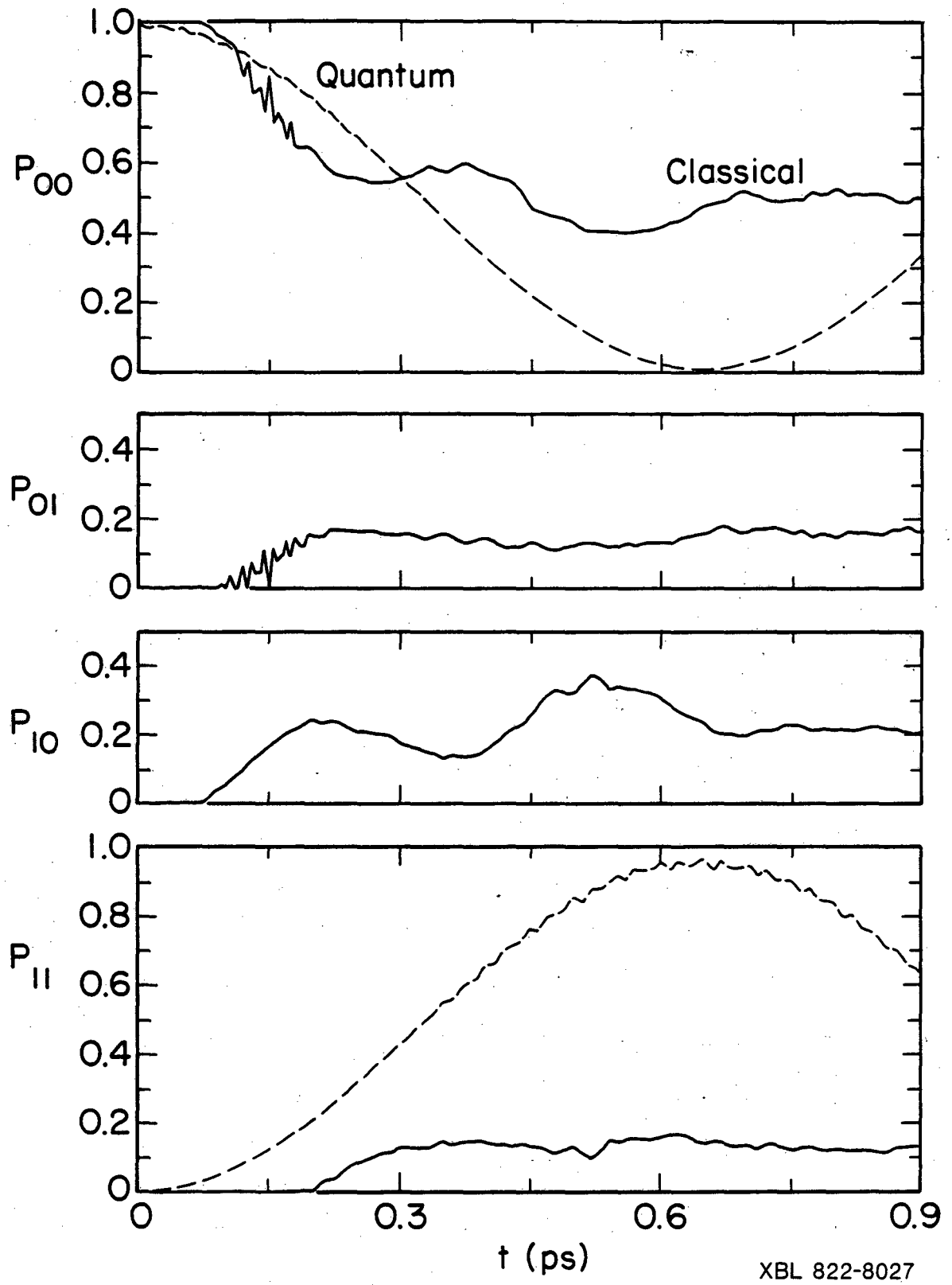
1.0
0.8
0.6
0.4
0.2
0
P_{00}
Quantum
Classical
0.4
0.2
0
P_{01}
0.4
0.2
0
P_{10}
1.0
0.8
0.6
0.4
0.2
0
P_{11}
0
0.3
0.6
0.9
t (ps)
XBL 822-8027

Figure 7

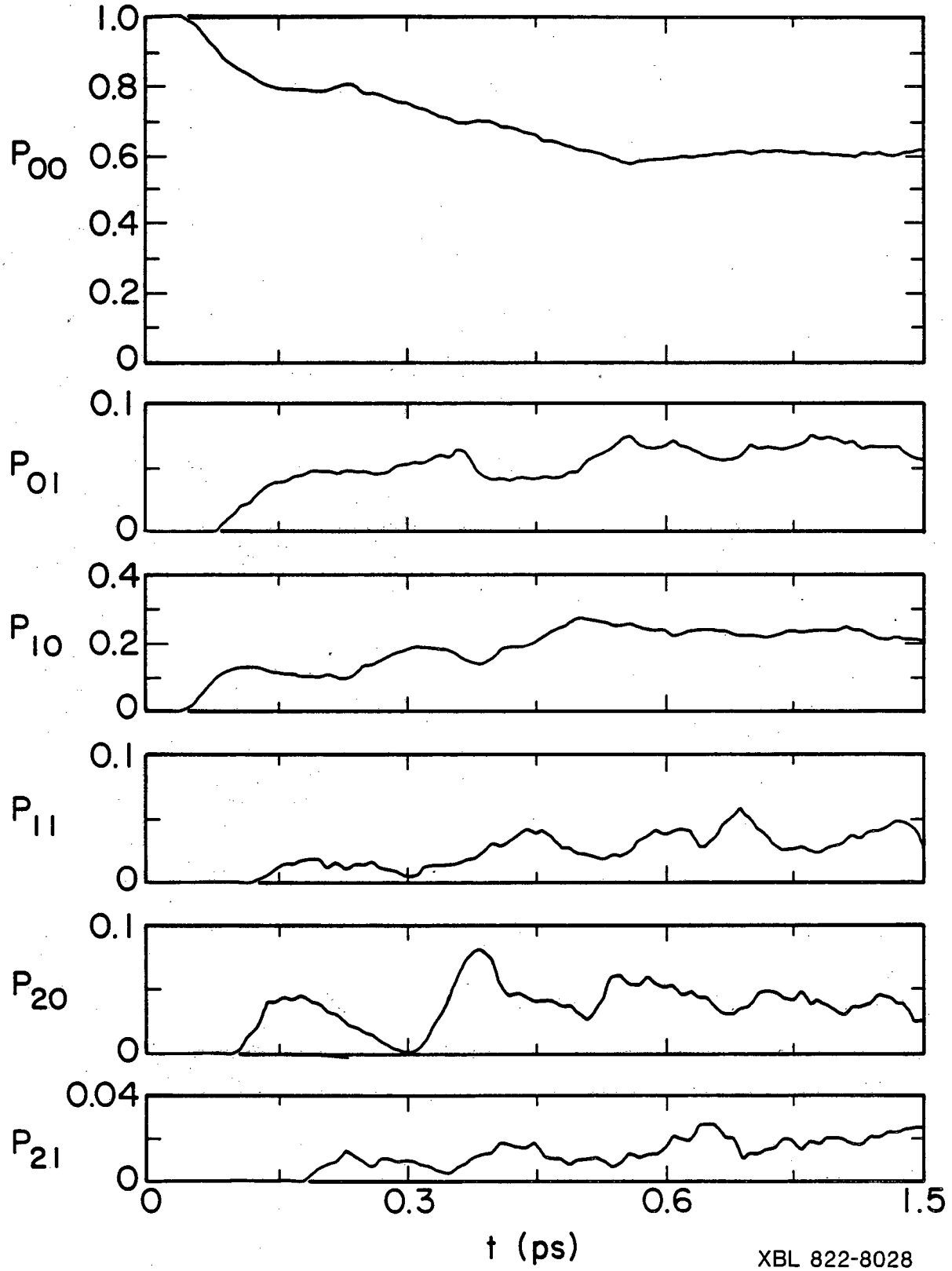
1.0
0.8
P_{00} 0.6
0.4
0.2
0
0.1
P_{01}
0
0.4
P_{10} 0.2
0
0.1
P_{11}
0
0.1
P_{20}
0
0.04
P_{21}
0
0
0.3
0.6
1.5
t (ps)
XBL 822-8028

Figure 8

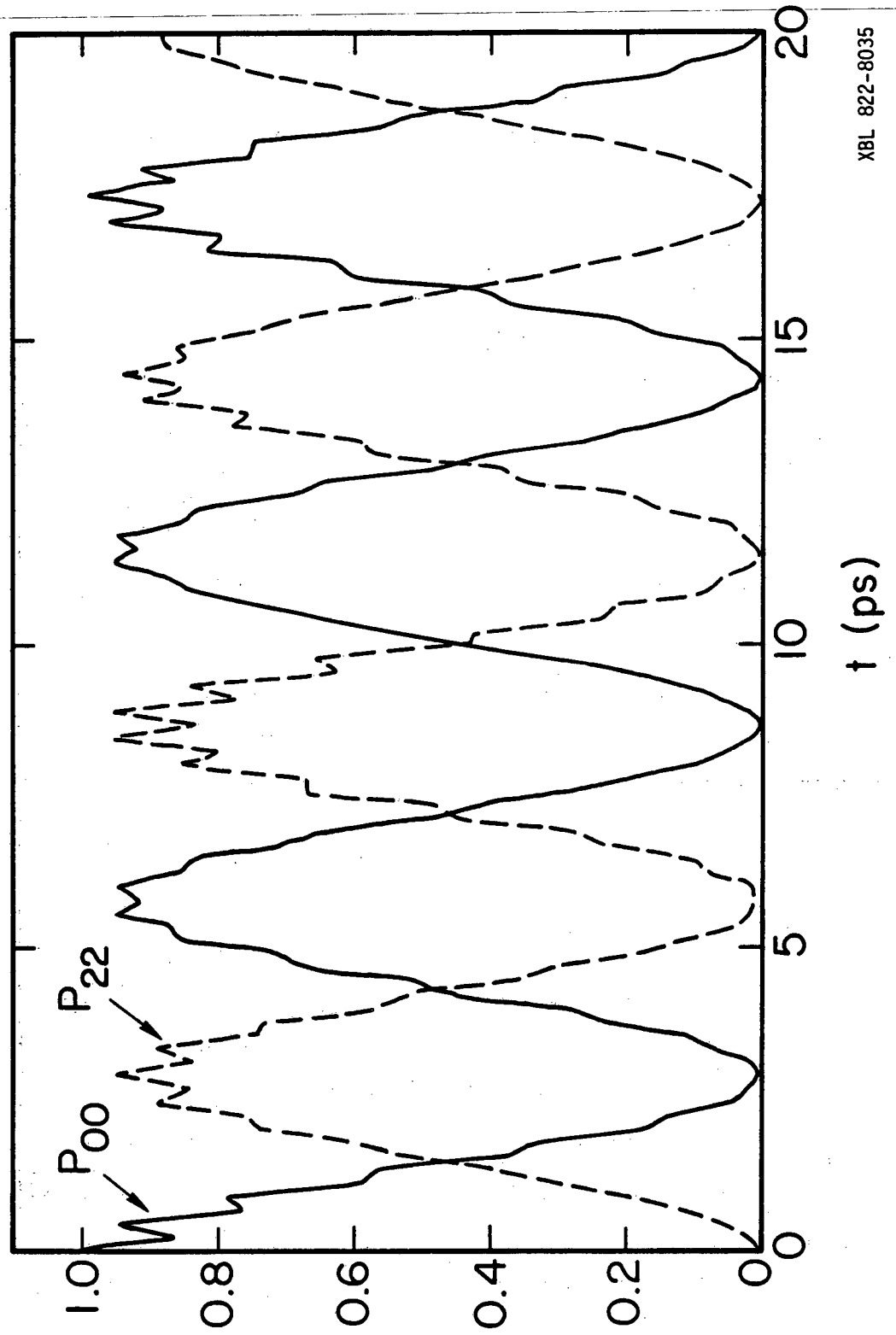

Figure 9

TECHNICAL INFORMATION DEPARTMENT
LAWRENCE BERKELEY LABORATORY
UNIVERSITY OF CALIFORNIA
BERKELEY, CALIFORNIA 94720